

Coordinated operation strategies for natural gas and power systems in presence of gas-related flexibilities

eISSN 2516-8401
 Received on 10th December 2018
 Revised 9th January 2019
 Accepted on 15th January 2019
 E-First on 28th February 2019
 doi: 10.1049/iet-esi.2018.0047
 www.ietdl.org

Hossein Ameli¹ ✉, Meysam Qadrdan², Goran Strbac¹

¹Control and Power group, Imperial College London, SW7 2AZ, UK

²Institute of Energy, Cardiff University, CF24 3AA, UK

✉ E-mail: h.ameli14@imperial.ac.uk

Abstract: A detailed investigation of the interaction between natural gas and power systems is necessary, due to the increasing interdependency of these vectors, especially in the context of renewable generations integration growth into the grid. In this study, an outer approximation with an equality relaxation decomposition method is proposed to solve a mixed-integer non-linear problem representing the operation of coupled natural gas and power systems. The proposed coupled modelling of natural gas and power systems is compared to decoupled operational modelling. It is demonstrated that operating gas and electricity as a coupled system resulted in about 7% of operational cost savings. In addition, the value of gas-related flexibility options, including flexible gas compressors, flexible gas generation plants, and gas interconnections, to the operation of natural gas and power systems is quantified for a 2030 GB energy system. It is shown that if the natural gas and power systems are flexible enough, the operation of the systems in the decoupled approach is almost the same as the coupled model and therefore there is no need to reform the current energy market framework to make the systems fully coupled.

Nomenclature

Parameters and variables

A	cross-sectional area of the pipe (m ²)
C	cost (£)
CR^{\max}	compressor pressure ratio
D	diameter of the pipe (mm)
e	emissions (tonnes)
f	friction factor
L	linepack (m ³)
Le	length of pipe (m)
M	incident matrix
p	pressure (Pascal)
p^{std}	pressure at standard condition (≈ 1 bar)
P	power output (MW)
r	reserve provided through a generation unit (MW)
R	gas constant for natural gas (518 J/kg K)
Re	Reynolds number
ts	time step
T_g	gas temperature (K)
T_g^{std}	gas temperature at standard condition (288 K)
Q	gas flow rate (m ³ /h)
v	velocity of gas along the pipe (m/s)
V	volume of gas (m ³)
w^{sd}	shut-down cost function (£)
w^{su}	start-up cost function (£)
X	objective function (£)
Z	compressibility factor (0.95)
β	polytropic exponent of a gas compressor (4.70 MJ/m ³)
η^{comp}	efficiency of compressor units (60%)
η^{pipe}	pipe efficiency factor (92%)
γ	On/Off state of generation units (1/0)
μ	gas turbine fuel rate coefficient of a compressor (0.084 m ³ /MJ)
μ_p	dynamic viscosity of gas (poise)
∂L	changes in linepack (m ³)
Ψ	maximum ramp up/down power of a generation unit (MW/h)

ω	proportion of wind for reserve requirements
ρ	density of gas (kg/m ³)
Θ	minimum up time of a generation unit (h)
$\underline{\Theta}$	minimum down time of a generation unit (h)
$\zeta_{c,t}$	amount of gas tapped by a compressor at node c and time t (m ³ /h)

Superscripts

avg	average
comp	compressor
cop	coupled
dis	discharge
ecomp	electrically-driven compressor
em	emissions
eload	electrical load
eshed	electrical load shedding
gload	gas load
gshed	gas load shedding
gstor	gas storage facility
inj	injection
min	minimum
max	maximum
std	standard
suc	suction
supp	supply
ur	unserved reserve
with	withdraw
var	variable

Sets

\mathcal{B}	set of busbars
\mathcal{C}	set of compressor nodes
\mathcal{C}_e	set of electrically-driven compressors
\mathcal{G}	set of generation units
\mathcal{H}	set of thermal generation units
\mathcal{L}_g	set of gas pipelines
\mathcal{N}	set of nodes
\mathcal{P}	set of pump units
\mathcal{S}_g	set of gas storage facilities

\mathcal{T} time horizon (h)
 \mathcal{W} set of flows
 \mathcal{Y} set of gas terminals

1 Introduction

1.1 Interaction between natural gas and power systems

In GB, natural gas supplies a substantial amount of energy used for heating (278 TWh in 2014) and power generation (218 TWh in 2014) [1]. Despite the increasing share of renewable and low carbon energy sources of power and heat production, it is expected that natural gas will continue to be an important part of the energy mix to 2030 [2].

Gas demand for power generation will be affected by the increase in wind and photovoltaic generation. Owing to their flexible operating characteristics, gas-fired generating units will play a crucial role in compensating for the variability of renewable energy sources. Consequently, variations of wind and solar generation will be transferred to the gas demand [3], which makes the operation of these systems more interdependent. As a result, investigating a coordinated operation of these systems is of great importance.

The interactions of natural gas and power systems are studied in the literature in detail [4–13]. A security-constrained unit commitment model considering natural gas transmission constraints is proposed in [4, 5]. In this model, the scheduling problem of gas and electricity systems is solved using an iterative approach, i.e. the power system optimal dispatch problem was solved first and then gas demand for electricity generation was used in the gas network model for a feasibility check. In [7], a coupled model of natural gas and power systems is presented to account for the adequacy of gas as a fuel to power stations in the power system reliability assessment. In [8], the efficiency of the coordinated operation of natural gas and power systems in the presence of microgrid aggregators is quantified. In [10], two different coupling methodologies for gas and electricity markets based on (a) maximising the profit of electricity market, and (b) minimising the operational cost of the natural gas system are presented. It was shown that if the modelling is accurate, the difference between these two methodologies may be negligible. Clegg and Mancarella [12] proposed an iterative operation of natural gas and power systems without unit commitment (UC) constraints to investigate the benefits of storing renewable electricity in the form of hydrogen and methane.

1.2 Solution algorithms for the coupled operation of natural gas and power systems

The optimisation problem for the coordinated operation of coupled natural gas and power systems is a mixed integer non-linear programming (MINLP), due to binary variables in the UC constraints of generating units and non-linear equations in natural gas system dynamics.

MINLP problem is a complicated and challenging class from theoretical, algorithmic and computational perspectives [14, 15]. To simplify the complexity of solving the MINLP problem, several algorithms such as generalised benders decomposition (GBD), outer approximation (OA), feasibility approach, OA with equality relaxation (OA/ER), generalised OA, and generalised cross decomposition are developed [14]. A number of previous works have applied deterministic and meta-heuristic solution techniques to solve MINLP problems [15–25]. Deterministic methods such as priority list [16], branch and bound (BB) [17], Lagrangian relaxation (LR) [18], and benders decomposition (BD) [22] have been applied to solve MINLP problems. The BB method is suitable for problems with a small number of variables. The LR method is an appropriate method for large-scale systems. However, due to the non-zero duality gap, the solution obtained from the dual problem could be infeasible [20]. In power systems, there are several studies that applied BD such as [22] in the UC problem. To solve the UC problems, heuristic methods such as evolutionary algorithm [23] and particle swarm optimisation [25] have been implemented. In these methods, the optimal solution can be achieved if the

optimality is obtained at each iteration. However, due to the stochastic nature of the search algorithms, the weakness of these methods is that mostly optimality of the solution cannot be guaranteed and consequently evaluating a solution is difficult. In addition, there are studies that linearise the non-linear constraints to make the problem mixed-integer linear programming (MILP) [26]. The OA approach is applied in a few studies for solving the UC problem [27, 28].

In the context of coordination of gas and electricity systems, in [29], optimal operation of natural gas and power systems in the presence of a large capacity of wind was assessed through a combined gas and electricity network (CGEN) model. In this model, to avoid computational complexity, UC constraints were not taken into account. The CGEN model was further improved in [30] by taking into account the unit commitment constraints of thermal generating units. In [7], in the coupled model of natural gas and power systems, non-linear equations are linearised, and therefore the model is formulated as a MILP. In [11], static and dynamic gas flow modelling are considered for the gas system operation. The results indicate the security and economic efficiency enhancement of the dynamic model. In the proposed model, the unit commitment constraints for thermal generating units are neglected in order to reduce the complexity of the optimisation problem. Deane *et al.* [31] formulated a MILP problem to analyse gas supply interruption cases in an integrated electricity and gas system. In another study [32], a co-optimisation scheduling of natural gas and power systems is proposed. A decomposition method is implemented to solve separately the gas network sub-problem and electricity network sub-problem.

1.3 Key contributions of this work

For the operation of natural gas and power systems, two different strategies are compared: (a) decoupled approach in which these systems are operated in an iterative manner and (b) coordinated operation of coupled natural gas and power systems. The value of the coupled modelling is quantified through comparing with the decoupled approach. Due to the nature of the non-linear equations in the natural gas system, the MINLP problem of coordinated operation of coupled natural gas and power systems is non-convex, which implies the potential existence of local optimums. Therefore, one of the contributions of this research is to propose an efficient solution algorithm for the optimisation problem representing the coupled operation of natural gas and power systems. To the best of our knowledge, for the first time, an OA/ER decomposition method is implemented to solve the optimisation problem of integrated gas and electricity systems operation. Moreover, as the second contribution of this research, the role of gas-related flexibility options including: (a) multi-directional compressors, (b) flexible gas plants, and (c) gas interconnections, in the interaction between these systems is investigated. A set of case studies are analysed on a 2030 GB gas and electricity transmission system to compare the proposed modelling approaches, and to quantify the value of gas-related flexibility options in interdependency of natural gas and power systems in the presence of renewables.

2 Operational models for natural gas and power systems

Operation of the natural gas and power systems is optimised using a day-ahead rolling strategy. A complete set of equations used in the model is provided.

2.1 Operation of natural gas system

2.1.1 Gas flow along a pipe: In the gas flow model, it is assumed that gas flows in one dimension, as the variations of gas properties along the radius are much lower than variations in the pipeline direction. In light of this, the following conditions are assumed: (a) pipe is horizontal, (b) along the pipe the velocity and temperature are constant, (c) pipe's diameter is small compared to the radius of curvature, and (d) change of cross-sectional area along the path of gas stream is negligible [6].

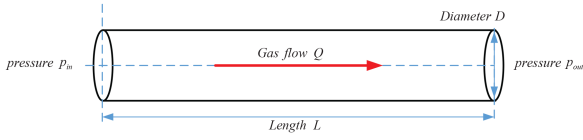


Fig. 1 Gas flow along a pipe

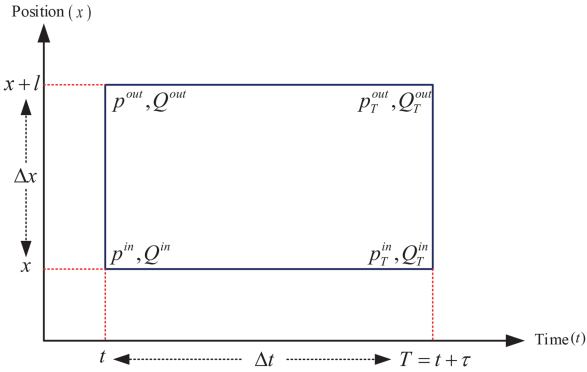


Fig. 2 Finite difference cell

The gas flow along a pipe (Fig. 1) is calculated through continuity (1) and momentum (2) equations [33]. The volumetric flow rate of the gas is governed by (3)

$$\frac{\partial Q}{\partial x} = -\frac{A}{\rho ZRT_g} \cdot \frac{\partial p}{\partial t}, \quad (1)$$

$$\frac{\partial p}{\partial x} = -\frac{\partial \rho v}{\partial t} - \frac{\partial \rho v^2}{\partial x} - \frac{2f\rho \cdot v^2}{D}, \quad (2)$$

$$Q = v \cdot A. \quad (3)$$

Through neglecting terms of $(\partial \rho v^2 / \partial x)$ and $(\partial \rho v / \partial t)$ due to the gas flow slow changes and large time steps (hourly compared to seconds) [6], in combination with (3), and mass flow rate (4), the transient flow of gas through a horizontal pipe is described in (5)

$$M = \rho \cdot Q = \rho^{\text{std}} \cdot Q^{\text{std}}, \quad (4)$$

$$\frac{\partial p}{\partial x} = -\frac{2f\rho^{\text{std}} \cdot Q^{\text{std}} |Q^{\text{std}}|}{A^2 D}, \quad (5)$$

where M is the mass flow rate (kg/s); ρ^{std} is the density of gas under standard conditions ($0.713 \text{ m}^3/\text{s}$); and Q^{std} is the volumetric flow rate under standard conditions (m^3/s).

In order to represent the derivatives of (1) and (5), a finite difference approach is applied [6]. Fig. 2 illustrates the time-position plane of a pipeline element. In this figure, l is a length of the pipeline and τ is the time step of the modelling. The steady-state average pressure of a pipeline and the average gas flow in a pipeline are formulated in (6) and (7)

$$p_T^{\text{avg}} = \frac{1}{2}(p_T^{\text{in}} + p_T^{\text{out}}), \quad (6)$$

$$Q_T^{\text{avg}} = \frac{1}{2}(Q_T^{\text{in}} + Q_T^{\text{out}}). \quad (7)$$

By applying (6) and (7) and the gas equation of state (8) [33], (1) and (5) are converted to ordinary differential equations used for calculating gas flow through a pipe (9) and (10)

$$Z \cdot R = \frac{p}{\rho \cdot T_g} = \frac{p^{\text{std}}}{\rho \cdot T_g^{\text{std}}}, \quad (8)$$

$$\frac{Q_T^{\text{out, std}} - Q_T^{\text{in, std}}}{\Delta x} = -\frac{A}{\rho^{\text{std}} ZRT_g} \cdot \frac{p_T^{\text{avg}} - p^{\text{avg}}}{\Delta t}, \quad (9)$$

$$\frac{p_T^{\text{out}} - p_T^{\text{in}}}{\Delta x} = -\frac{2f(\rho^{\text{std}})^2 ZRT_g \cdot Q_T^{\text{avg, std}} |Q_T^{\text{avg, std}}|}{A^2 D \cdot p_T^{\text{avg}}}. \quad (10)$$

In this research, the Panhandle A approach for high-pressure networks [33] for gas flow is implemented. Therefore, the friction factor is defined as (11) [33]

$$\sqrt{\frac{1}{f}} = 6.872 \cdot (Re)^{0.073} \cdot \eta^{\text{pipe}}, \quad (11)$$

$$Re = \frac{\rho \cdot v \cdot D}{\mu_p}. \quad (12)$$

On the other side, the gas flow could be calculated as follows (13):

$$Q = A \cdot v = \frac{\pi D^2}{4} v \quad (13)$$

$$\Rightarrow v = \frac{4Q\rho}{\pi D^2}. \quad (14)$$

By substituting (13) into (12), (15) is obtained, and by assuming the physical parameters of gas are constant, (16) is achieved

$$Re = \frac{4Q\rho}{\mu_p D \pi}, \quad (15)$$

$$Re = B \frac{Q}{D}, \quad (16)$$

where B is constant. Thus, through combining (16) to (11), the friction factor is simplified (17)

$$\sqrt{\frac{1}{f}} = 6.872 \cdot C^{0.073} \cdot \frac{Q^{0.073} \cdot \eta^{\text{pipe}}}{D^{0.073}}. \quad (17)$$

In a natural gas network, (10) can be written as (18)

$$\forall l \in \mathcal{L}_g, t \in \mathcal{T}: \frac{p_{l,t}^{\text{out}} - p_{l,t}^{\text{in}}}{L_{e_l}} = -\frac{2f(\rho^{\text{std}})^2 ZRT_g \cdot Q_{l,t}^{\text{avg}} |Q_{l,t}^{\text{avg}}|}{A^2 D \cdot \left(\frac{1}{2}(p_{l,t}^{\text{out}} + p_{l,t}^{\text{in}})\right)}. \quad (18)$$

Finally, by substituting (17) into (18) and simplification, (19) would be achieved

$$\forall l \in \mathcal{L}_g, t \in \mathcal{T}: h_{l,t}^{\text{flow}}: (p_{l,t}^{\text{in}})^2 - (p_{l,t}^{\text{out}})^2 = \frac{18.43 L_{e_l}}{(\eta_l^{\text{pipe}})^2 \cdot D_l^{4.854}} Q_{l,t}^{\text{avg}} |Q_{l,t}^{\text{avg}}|^{0.854}. \quad (19)$$

2.1.2 Gas compressors: In order to enhance the lost pressure caused by friction in the pipelines, the installation of compressor units is considered. The required power of the prime mover for the compressor is calculated by (20) [6]. The ratio of discharge pressure to suction pressure is limited to (21). Each compressor is subjected to a maximum flow rate, maximum power consumption, and maximum pressure constraints [34]. The tapped gas is calculated from (22)

$$\forall c \in \mathcal{C}, t \in \mathcal{T}: h_{c,t}^{\text{comp}}: P_{c,t}^{\text{comp}} = \frac{\beta \cdot Q_{c,t}^{\text{comp}}}{\eta^{\text{comp}}} \cdot \left[\left(\frac{p_{c,t}^{\text{dis}}}{p_{c,t}^{\text{suc}}} \right)^{(1/\beta)} - 1 \right], \quad (20)$$

$$1 \leq \frac{p_{c,t}^{\text{dis}}}{p_{c,t}^{\text{suc}}} \leq CR^{\text{max}}, \quad (21)$$

$$\zeta_{c,t} = \mu \cdot P_{c,t}^{\text{comp}}. \quad (22)$$

2.1.3 Linepack: Due to the fact that supplying gas from sources take time to reach demand centres (typically hours), linepack [34] is used to meet the rapid changes in the network. The linepack L within a pipe, calculated through combining (8), (23), (24), and considering parameter K as in (25), is shown in (26)

$$V = \rho^{-1}, \quad (23)$$

$$p^{\text{avg}} \cdot V = p^{\text{std}} \cdot V^{\text{std}}, \quad (24)$$

$$K = \frac{V}{\rho \cdot Z \cdot R \cdot T_g^{\text{std}}} = \frac{A \cdot Le}{\rho \cdot Z \cdot R \cdot T_g^{\text{std}}}, \quad (25)$$

$$L = V^{\text{std}} = K \cdot p^{\text{avg}}. \quad (26)$$

In the dynamic state, gas flow oscillates when supply or demand changes. Change of total gas volume due to the mass conservation law is equal to the difference between flow into and out of the pipe (27)

$$\forall l \in \mathcal{L}_g, t \in \mathcal{T}: L_{l,t} = L_{l,t-1} + \underbrace{\int_{t-1}^t (Q_{l,\tau-1}^{\text{in}} - Q_{l,\tau-1}^{\text{out}}) \cdot d\tau}_{\partial L_{l,t}}. \quad (27)$$

To deal with the integration as a non-linear function in (27), the changes in the gas flow are replaced with the changes in pressure through using (3), and therefore (27) can be approximated to (28)

$$\forall l \in \mathcal{L}_g, t \in \mathcal{T}: h_{l,t}^{\text{linepack}}: L_{l,t} = L_{l,t-1} + K(l) \cdot (p_{l,t}^{\text{avg}} - p_{l,t-1}^{\text{avg}}). \quad (28)$$

2.1.4 Natural gas system constraints: Pressure limits (29) and the gas flow balance (30) (i.e. gas inflows are balanced with gas outflows) are imposed on each system node

$$\forall x \in \mathcal{M}, t \in \mathcal{T}: p_x^{\text{min}} \leq p_{x,t} \leq p_x^{\text{max}}, \quad (29)$$

$$\begin{aligned} Q_{x,t}^{\text{supp}} + \Delta Q_{x,t}^{\text{gstor}} + \sum_{w \in \mathcal{W}} M_{w,x}^{\text{flow}} \cdot Q_{w,t} + \sum_{c \in \mathcal{C}} M_{c,x}^{\text{comp}} \cdot Q_{c,t} \\ = Q_{x,t}^{\text{load}} + Q_{x,t}^{\text{gen}} - Q_{x,t}^{\text{gshed}} + \sum_{c \in \mathcal{C} - \mathcal{C}_e} M_{c,x}^{\text{ecomp}} \cdot \zeta_{c,t}. \end{aligned} \quad (30)$$

2.2 Power system modelling

The general formulation of the power flow model (based on the DC power flow model [35]) is applied to represent the power system (31)–(33). Hourly system demand–supply balance constraints (31) and the hourly network lines' capacity constraint (32). The power flow through the transmission line is calculated through (33)

$$\forall t \in \mathcal{T}: \sum_{i \in \mathcal{N}_s} s_{i,t} - \sum_{j \in \mathcal{N}_d} d_{j,t} = 0, \quad (31)$$

$$\forall l \in \mathcal{L}_e, t \in \mathcal{T}: F_{l,t} \leq |F_l^{\text{cap}}|, \quad (32)$$

$$F_{l,t} = \sum_{i \in \mathcal{N}_s} h_{l,i}^s \cdot s_{i,t} - \sum_{j \in \mathcal{N}_d} h_{l,j}^d \cdot d_{j,t}. \quad (33)$$

where \mathcal{L}_e is the set of electricity transmission lines; \mathcal{N}_s is the set of supply points; \mathcal{N}_d is the set of demand points; $s_{i,t}$ is the power supply at location i and time t ; $d_{j,t}$ is the power demand at location j and time t ; F_l^{cap} is the maximum capacity of line l (MW); $F_{l,t}$ is the power flow of line l and time t (MW); $h_{l,i}^s$ is the sensitivity coefficient of flow on line l with respect to power injection of supply point i (based on DC load flow model); $h_{l,j}^d$ is the sensitivity coefficient of flow on line l with respect to power demand at location j (based on the DC load flow model).

The generation technologies characteristics including, physical limitations (34), state of the unit (On/Off) (35), reserve provision (36), minimum up/down time (37) and (38) [36], ramp up/down limits (39), start-up cost (40) and shut-down cost (41), spinning reserve, and power flow balance at each time step (43) is considered in the modelling of the power system

$$\forall i \in \mathcal{G} - \mathcal{H}, t \in \mathcal{T}: P_i^{\text{min}} \leq P_{i,t} \leq P_i^{\text{max}}, \quad (34)$$

$$\forall i \in \mathcal{H}, t \in \mathcal{T}: P_{i,t} \geq \gamma_{i,t} \cdot P_i^{\text{min}}, \quad (35)$$

$$P_{i,t} + r_{i,t} \leq \gamma_{i,t} \cdot P_i^{\text{max}}, \quad (36)$$

$$\gamma_{i,t'} - \gamma_{i,t'-1} \leq \gamma_{i,t}; \quad t' = [t - \bar{\Theta}_i + 1, t - 1], \quad (37)$$

$$\gamma_{i,t'-1} - \gamma_{i,t'} \leq 1 - \gamma_{i,t}; \quad t' = [t - \underline{\Theta}_i + 1, t - 1], \quad (38)$$

$$|P_{i,t} - P_{i,t-1}| \leq \Psi_i, \quad (39)$$

$$w_{i,t}^{\text{su}} = C_i^{\text{su}} \cdot \max\{\gamma_{i,t} - \gamma_{i,t-1}, 0\}, \quad (40)$$

$$w_{i,t}^{\text{sd}} = C_i^{\text{sd}} \cdot \max\{\gamma_{i,t-1} - \gamma_{i,t}, 0\}, \quad (41)$$

$$ur_t + \sum_{i \in \mathcal{H}} r_{i,t} + \sum_{p \in \mathcal{P}} r_{i,t}^{\text{pump}} \geq \max_{i \in \mathcal{H}} (P_i^{\text{max}}) + \omega \cdot \sum_{b \in \mathcal{B}} P_{b,t}^{\text{wind}}, \quad (42)$$

$$\begin{aligned} \forall t \in \mathcal{T}: \sum_{i \in \mathcal{G}} P_{i,t} + \sum_{b \in \mathcal{B}} P_{b,t}^{\text{wind}} + \sum_{p \in \mathcal{P}} (P_{p,t}^{\text{pump,with}} - P_{p,t}^{\text{pump,inj}}) \\ = \sum_{b \in \mathcal{B}} (P_{b,t}^{\text{load}} - P_{b,t}^{\text{shed}} + P_{b,t}^{\text{ecomp}}). \end{aligned} \quad (43)$$

3 Operational strategies for natural gas and power systems

The model has perfect foresight on gas and electricity demand as well as available wind power within the same day. Each optimisation is conducted for a time horizon of 32 h, but the results for the first 24 h are only used. This is to avoid the 'end-of-optimisation' effect and model operation of energy storages and unit commitment of the thermal generators more realistically. After solving the optimisation problem for each iteration (i.e. 32-h), state of the system, e.g. linepack, storage, On/Off state of thermal generating units for first 24-h of the iteration are stored. Afterwards, the latter data is used in time-dependent constraints when running the model for the next 32-h. At each iteration, the first 24-h are taken as the solutions.

Two operation strategies are presented. The first strategy is a decoupled approach with an iterative process, in which operation of the power system is modelled irrespective to the natural gas system. Then, using the results from the optimisation of the power system, the operation of the natural gas system is optimised. The second strategy is an integrated approach, which takes into account every constraint of the natural gas and power systems, simultaneously.

3.1 Decoupled modelling

In the decoupled mode, the operation of the power system (including UC/economic dispatch and power flow) is optimised, hence gas demand for power generation is calculated. This method has been used in different manners in the literature such as in [34, 37]. In this approach, gas demand for power generation is provided as an input to the natural gas system operation model. In this modelling, operational costs of the power system are minimised, followed by minimisation of the operational costs of the natural gas system. In the power system operational model, costs of power generation, electrical load shedding, and greenhouse gas emission penalties are taken into account in the objective function (44). For the natural gas system, costs of gas supplies, storage facilities, changes of the linepack, and gas load shedding are considered (45)

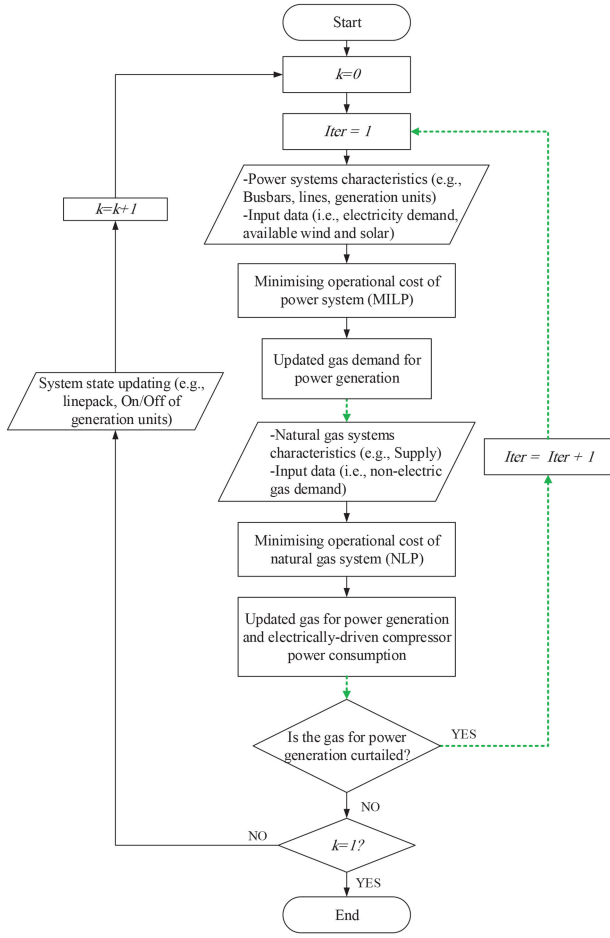


Fig. 3 Decoupled mode algorithm

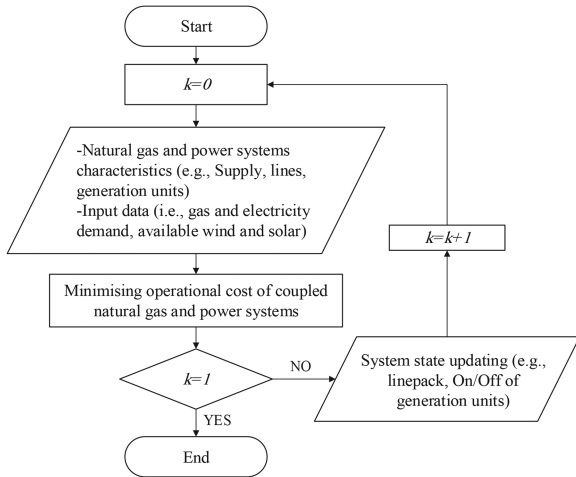


Fig. 4 Coupled mode algorithm

$$X_{elec} = \sum_{t=1}^T \left(\sum_{i \in \mathcal{G}} (C_i^{fuel} + C_i^{var}) \cdot P_{i,t} \cdot ts + \sum_{i \in \mathcal{K}} C_i^{em} \cdot e_{i,t} + C^{ur} \cdot ur_t \cdot ts + \sum_{b \in \mathcal{B}} C^{eshed} \cdot P_{b,t}^{eshed} \cdot ts + \sum_{i \in \mathcal{K}} (w_{i,t}^{su} + w_{i,t}^{sd}) \right), \quad (44)$$

$$X_{gas} = \sum_{t=1}^T \left(\sum_{s \in \mathcal{S}_g} (C^{gstor.with} \cdot Q_{s,t}^{gstor.with} - C^{gstor.inj} \cdot Q_{s,t}^{gstor.inj}) + \sum_{y \in \mathcal{Y}} C^{gas} \cdot Q_{y,t}^{supp} + \sum_{l \in \mathcal{L}_g} C^{gas} \cdot \partial L_{l,t} + \sum_{x \in \mathcal{M}} C^{gshed} \cdot Q_{x,t}^{gshed} \right). \quad (45)$$

The delivered gas for power generation as well as the power consumption of electrically-driven compressors are inputs of the operational model of the power system. If the total required gas for power generation cannot be delivered, re-dispatch of power is necessary to complement the lack of power generated by the gas plants. For this purpose, in the next iteration, a constraint is imposed to limit the maximum power generation from gas plants. This procedure is carried out to avoid infeasibility in the operation of the gas system.

The algorithm of decoupled modelling is demonstrated in Fig. 3. The green (dashed) lines indicate links of the natural gas and power systems. The decoupled approach does not consider gas supply constraints simultaneously when optimising the operation of the power system. Hence, a key disadvantage of this model is that the potential interruptions of gas supply do not affect the dispatch of gas-fired plants for the power system in the initial decision-making stage. Therefore, after providing the status of the delivered gas for power generation to the power system, it may be required to use more expensive options (e.g. interconnectors) or generating electricity from plants characterised with high emissions (e.g. coal plants), to keep energy balance in the power system.

3.2 Coupled modelling

In the coupled model, the natural gas and power systems constraints are considered simultaneously (Fig. 4). The coupled model minimises the total operational cost of natural gas and power systems (46)

$$X_{cop} = X_{elec} + X_{gas}, \quad (46)$$

(see (47)), where X_{cop} is the cost of coupled operation of natural gas and power systems.

The corresponding optimisation problem of the coupled model is solved through the proposed OA/ER decomposition method. The main reason for using the decomposition method is to improve the computational performance of the optimisation (compared to successive linear programming solver for MINLP problems in Xpress-IVE [38]). Moreover, the rolling approach has been implemented to reduce the size of the optimisation problem at each step. Based on the output of the steady state optimisation for the time period, initial values are given to all decision variables. In addition, the decision variables are scaled; therefore the order of magnitude values do not vary significantly. The latter procedures

$$X_{cop} = \sum_{t=1}^T \left(\underbrace{ur_t \cdot ts + \sum_{i \in \mathcal{G}} (C_i^{fuel} + C_i^{var}) \cdot P_{i,t} \cdot ts + \sum_{i \in \mathcal{K}} C_i^{em} \cdot e_{i,t} + \sum_{b \in \mathcal{B}} C^{eshed} \cdot P_{b,t}^{eshed} \cdot ts}_{\text{Continuous variables of power system: } f(P_t, P_t^{eshed}, e_t, ur_t)} + \underbrace{\sum_{i \in \mathcal{K}} (w_{i,t}^{su} + w_{i,t}^{sd})}_{\text{Binary variables of power system}} \right. \\ \left. + \underbrace{\sum_{y \in \mathcal{Y}} C^{gas} \cdot Q_{y,t}^{supp} + \sum_{s \in \mathcal{S}_g} (C^{gstor.with} \cdot Q_{s,t}^{gstor.with} - C^{gstor.inj} \cdot Q_{s,t}^{gstor.inj}) + \sum_{l \in \mathcal{L}_g} C^{gas} \cdot \partial L_{l,t} + \sum_{x \in \mathcal{M}} C^{gshed} \cdot Q_{x,t}^{gshed}}_{\text{Continuous variables of natural gas system: } g(Q_t^{supp}, Q_t^{gstor}, CL_t, Q_t^{gshed})} \right). \quad (47)$$

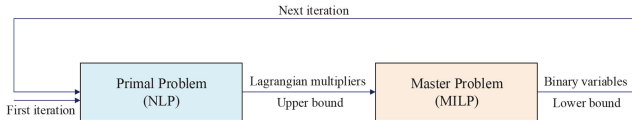


Fig. 5 Structure of the OA/ER decomposition method

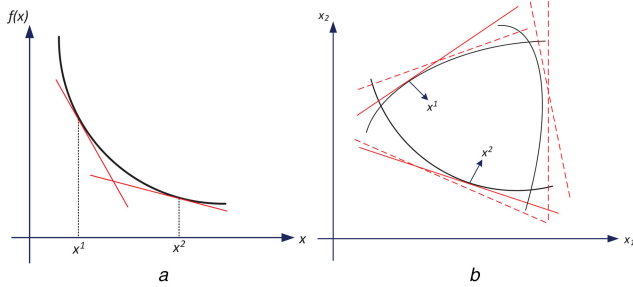


Fig. 6 Geometrical interpretation of linearisation in the master problem
(a) Underestimate objective function, (b) Overestimate feasible region [14]

are used to achieve convergence and stability in the optimisation process.

In general, in a decoupled approach model, since in an iterative process the systems are optimised, if the systems are linked properly, the results of this method should be very close to optimising the systems fully coupled. However, to obtain this accuracy, many iterations should be carried out, which makes the model computationally expensive. In this research, based on the criteria (gas load curtailment), the number of iterations can be up to two iterations. This means if gas load curtailment has not happened, after one iteration the optimisation will terminate, although the results are not necessary close to the coupled model.

Regarding the coupled model, in the next section, a decomposition method based on the OA/ER approach is introduced to solve effectively the problem of coupled operation of natural gas and power systems.

4 Solution algorithm for coupled operation of natural gas and power system

In this research, a solution algorithm is developed based on the OA/ER approach [14] considering penalties for solving the MINLP problem of the operation of coupled natural gas and power systems. The OA/ER handles with non-linear inequalities, and similar to GBD creates sequences of upper and lower bounds. As a difference between these methods, the GBD method uses dual information, while the OA/ER is based on using primal information. Compared to the GBD method, the advantage of OA/ER is that in problems with a large number of binary variables, fewer iterations are required to reach the convergence. However, due to the number of constraints added per iteration in the master problem, computational time for solving the master problem in OA/ER is more than that of GBD [39].

4.1 Basic theory

In OA/ER, to solve the MINLP problem, for every iteration, an upper bound and a lower bound of the objective value are generated. In Fig. 5, the structure of the OA/ER method is shown. Upper bound is obtained from the primal problem, while lower bound is obtained from the master problem. In the primal problem, binary variables are fixed. The Lagrangian multipliers associated with the non-linear equality constraints and the upper bound are supplied from the primal to solve the master problem. In the master problem, the non-linear equalities are relaxed into linear inequalities using the Lagrangian multipliers provided from the primal problem. The solution of the master problem provides information for the lower bound, and the fixed binary variables carried out in the next iteration of the primal problem. As the iterations proceed, it is shown that upper bounds and lower bounds sequences converge in a finite number of iterations.

For better understanding, an example of a geometrical interpretation of the master problem in OA with a convex objective function and the convex feasible region is presented in Fig. 6. As is presented, the convex objective function is being underestimated, and through these linearisations, the convex feasible region is overestimated (further details can be found in [14, 39]).

4.2 Objective function

The objective function for the problem is the operation cost of coupled natural gas and power systems (46), which can be formulated as (47), where

P_t set of $P_{i,t}$ at time t , $i \in \mathcal{G}$

P_t^{shed} set of $P_{b,t}^{\text{shed}}$ at time t , $b \in \mathcal{B}$

e_t set of $e_{i,t}$ at time t , $i \in \mathcal{K}$

Q_t^{supp} set of $Q_{y,t}^{\text{supp}}$ at time t , $y \in \mathcal{Y}$

Q_t^{gstor} set of $Q_{s,t}^{\text{gstor, inj}}$ and $Q_{s,t}^{\text{gstor, with}}$ at time t , $s \in \mathcal{S}_g$

CL_t set of $\partial L_{l,t}$ at time t , $l \in \mathcal{L}_g$

$Q_{x,t}^{\text{ghed}}$ set of $Q_{x,t}^{\text{ghed}}$ at time t , $x \in \mathcal{M}$

In the OA/ER approach for solving the optimisation problem of coupled operation of natural gas and power systems, the whole energy system constraints in both primal and master problems are taken into account, which will be expressed in the following section.

For sake of simplification, the cost associated with continuous variables is presented by X_{cont} . Hence, the objective function is presented as follows (48):

$$X_{\text{cop}} = X_{\text{cont}} + \sum_{t=1}^T \left(\sum_{i \in \mathcal{K}} (w_{i,t}^{\text{su}(\rho)} + w_{i,t}^{\text{sd}(\rho)}) \right). \quad (48)$$

4.3 Primal problem

As mentioned previously, in the primal problem, binary variables are fixed. Therefore, binary variables of $w_{i,t}^{\text{su}}$ and $w_{i,t}^{\text{sd}}$ functions in (47) are fixed, converting the problem to non-linear programming (NLP) (49), where $X_{\text{primal}}^{(\rho)}$ is the objective function of the primal problem at iteration ρ . The $(\cdot)^*$ in the equations represents a provided fixed value of the variables (i.e. initial value or output of one iteration of OA/ER)

$$X_{\text{primal}}^{(\rho)} = X_{\text{cont}} + \sum_{t=1}^T \left(\sum_{i \in \mathcal{K}} (w_{i,t}^{\text{su}(\rho)} + w_{i,t}^{\text{sd}(\rho)}) \right). \quad (49)$$

For the first iteration, initial values based on the decoupled approach are fed as an input to the primal problem ($w_{i,t}^{\text{su}(1)}$ and $w_{i,t}^{\text{sd}(1)}$). For the next iteration of the primal problem, information on binary variables is provided subsequently by the master problem.

Depending on the fixation of $w_{i,t}^{\text{su}(\rho)}$ and $w_{i,t}^{\text{sd}(\rho)}$, the primal problem can be feasible or not.

4.3.1 Feasible primal problem: If at iteration ρ , the primal problem is feasible, then the solution of continuous variables in the natural gas and power systems as well as Lagrangian multipliers associated with non-linear equalities would be provided for the master problem.

4.3.2 Infeasible primal problem: If at iteration ρ , the primal problem is infeasible, a penalty function associated with the binary variables is added to the objective function (50). A feasible solution exists when the penalty function is zero

$$X_{\text{inf}}^{(\rho)} = X_{\text{primal}}^{(\rho)} + \kappa \cdot \alpha \cdot \text{ts}. \quad (50)$$

Information on continuous variables in the power system $f(\mathbf{P}_t^{*(\rho)}, \mathbf{P}_t^{\text{shed}*(\rho)}, \mathbf{e}_t^{*(\rho)}, \mathbf{ur}_t^{*(\rho)})$ and in the natural gas system $g(\mathbf{Q}_t^{\text{supp}*(\rho)}, \mathbf{Q}_t^{\text{gstor}*(\rho)}, \mathbf{CL}_t^{*(\rho)}, \mathbf{Q}_t^{\text{gshed}*(\rho)})$ as well as the Lagrangian multipliers associated with natural gas system non-linear equations $\lambda_{x,t}^{\text{flow}(\rho)}$, $\lambda_{x,t}^{\text{comp}(\rho)}$, and $\lambda_{x,t}^{\text{linepack}(\rho)}$ are found from solving of the primal problem. Subsequently, the elements of $\Phi_{x,t}^{\text{flow}(\rho)}$, $\Phi_{x,t}^{\text{comp}(\rho)}$, and $\Phi_{x,t}^{\text{linepack}(\rho)}$ are calculated as follows (51)–(53). These elements are inputs to the master problem for converting the non-linear qualities to linear inequalities

$$\forall l \in \mathcal{L}_g, t \in \mathcal{T}: \phi_{l,t}^{\text{flow}(\rho)} = \begin{cases} -1 & \text{if } \lambda_{l,t}^{\text{flow}(\rho)} < 0 \\ +1 & \text{if } \lambda_{l,t}^{\text{flow}(\rho)} > 0 \\ 0 & \text{if } \lambda_{l,t}^{\text{flow}(\rho)} = 0 \end{cases}, \quad (51)$$

$$\forall c \in \mathcal{C}, t \in \mathcal{T}: \phi_{c,t}^{\text{comp}(\rho)} = \begin{cases} -1 & \text{if } \lambda_{c,t}^{\text{comp}(\rho)} < 0 \\ +1 & \text{if } \lambda_{c,t}^{\text{comp}(\rho)} > 0 \\ 0 & \text{if } \lambda_{c,t}^{\text{comp}(\rho)} = 0 \end{cases}, \quad (52)$$

$$\forall l \in \mathcal{L}_g, t \in \mathcal{T}: \phi_{l,t}^{\text{linepack}(\rho)} = \begin{cases} -1 & \text{if } \lambda_{l,t}^{\text{linepack}(\rho)} < 0 \\ +1 & \text{if } \lambda_{l,t}^{\text{linepack}(\rho)} > 0 \\ 0 & \text{if } \lambda_{l,t}^{\text{linepack}(\rho)} = 0 \end{cases}. \quad (53)$$

4.4 Master problem

The master problem is expressed by (54)–(60). The objective function of the problem is to minimise $X_{\text{master}}^{(\rho)}$ (54). Variable ξ is constrained through the linearised objective function of the primal at solution points of continuous variables in the power system $f(\mathbf{P}_t^{*(\rho)}, \mathbf{P}_t^{\text{shed}*(\rho)}, \mathbf{e}_t^{*(\rho)}, \mathbf{ur}_t^{*(\rho)})$ and in the natural gas system $g(\mathbf{Q}_t^{\text{supp}*(\rho)}, \mathbf{Q}_t^{\text{gstor}*(\rho)}, \mathbf{CL}_t^{*(\rho)}, \mathbf{Q}_t^{\text{gshed}*(\rho)})$ (55)

$$X_{\text{master}}^{(\rho)} = \left(\sum_{t=1}^{\mathcal{T}} \sum_{i \in \mathcal{X}} (w_{i,t}^{\text{su}} + w_{i,t}^{\text{sd}}) \right) + \xi. \quad (54)$$

(see (55))

$$\forall \rho \in \mathcal{F}: \xi \geq \sum_{t=1}^{\mathcal{T}} \left(f^*(\mathbf{P}_t^{(\rho)}, \mathbf{P}_t^{\text{shed}(\rho)}, \mathbf{e}_t^{(\rho)}, \mathbf{ur}_t^{(\rho)}) + g^*(\mathbf{Q}_t^{\text{supp}(\rho)}, \mathbf{Q}_t^{\text{gstor.inj}(\rho)}, \mathbf{Q}_t^{\text{gstor.with}(\rho)}, \mathbf{CL}_t^{(\rho)}, \mathbf{Q}_t^{\text{gshed}(\rho)}) \right. \\ \left. + [\nabla f^*(\mathbf{P}_t^{(\rho)}, \mathbf{P}_t^{\text{shed}(\rho)}, \mathbf{e}_t^{(\rho)}, \mathbf{ur}_t^{(\rho)})]^T \begin{bmatrix} \mathbf{P}_t - \mathbf{P}_t^{(\rho)} \\ \mathbf{P}_t^{\text{shed}} - \mathbf{P}_t^{\text{shed}(\rho)} \\ \mathbf{e}_t - \mathbf{e}_t^{(\rho)} \\ \mathbf{ur}_t - \mathbf{ur}_t^{(\rho)} \end{bmatrix} \right. \\ \left. + [\nabla g^*(\mathbf{Q}_t^{\text{supp}(\rho)}, \mathbf{Q}_t^{\text{gstor.inj}(\rho)}, \mathbf{Q}_t^{\text{gstor.with}(\rho)}, \mathbf{CL}_t^{(\rho)}, \mathbf{Q}_t^{\text{gshed}(\rho)})]^T \begin{bmatrix} \mathbf{Q}_t^{\text{supp}} - \mathbf{Q}_t^{\text{supp}(\rho)} \\ \mathbf{Q}_t^{\text{gstor.inj}} - \mathbf{Q}_t^{\text{gstor.inj}(\rho)} \\ \mathbf{Q}_t^{\text{gstor.with}} - \mathbf{Q}_t^{\text{gstor.with}(\rho)} \\ \mathbf{CL}_t - \mathbf{CL}_t^{(\rho)} \\ \mathbf{Q}_t^{\text{gshed}} - \mathbf{Q}_t^{\text{gshed}(\rho)} \end{bmatrix} \right), \quad (55)$$

$$\forall \rho \in \mathcal{F}, c \in \mathcal{C}, t \in \mathcal{T}: \Phi_{c,t}^{\text{comp}(\rho)} \\ \times \left(h_{c,t}^{\text{comp}*(\rho)} (\mathbf{Q}_{c,t}^{\text{comp}(\rho)}, p_{c,t}^{\text{dis}(\rho)}, p_{c,t}^{\text{suc}(\rho)}) + [\nabla h_{c,t}^{\text{comp}*(\rho)} (\mathbf{Q}_{c,t}^{\text{comp}(\rho)}, p_{c,t}^{\text{dis}(\rho)}, p_{c,t}^{\text{suc}(\rho)})]^T \begin{bmatrix} \mathbf{Q}_{c,t}^{\text{comp}} - \mathbf{Q}_{c,t}^{\text{comp}(\rho)} \\ p_{c,t}^{\text{suc}} - p_{c,t}^{\text{suc}(\rho)} \\ p_{c,t}^{\text{dis}} - p_{c,t}^{\text{dis}(\rho)} \end{bmatrix} \right) \leq 0, \quad (57)$$

$$\forall \rho \in \mathcal{F}, l \in \mathcal{L}_g, t \in \mathcal{T}: \Phi_{l,t}^{\text{flow}(\rho)} \\ \times \left(h_{l,t}^{\text{flow}*(\rho)} (p_{l,t}^{\text{in}(\rho)}, p_{l,t}^{\text{out}(\rho)}, \mathbf{Q}_{l,t}^{\text{avg}(\rho)}) + [\nabla h_{l,t}^{\text{flow}*(\rho)} (p_{l,t}^{\text{in}(\rho)}, p_{l,t}^{\text{out}(\rho)}, \mathbf{Q}_{l,t}^{\text{avg}(\rho)})]^T \right. \\ \left. \times \begin{bmatrix} p_{l,t}^{\text{in}} - p_{l,t}^{\text{in}(\rho)} \\ p_{l,t}^{\text{out}} - p_{l,t}^{\text{out}(\rho)} \\ \mathbf{Q}_{l,t}^{\text{avg}} - \mathbf{Q}_{l,t}^{\text{avg}(\rho)} \end{bmatrix} \right) \leq 0, \quad (56)$$

(see (57))

$$\forall \rho \in \mathcal{F}, l \in \mathcal{L}_g, t \in \mathcal{T}: \Phi_{l,t}^{\text{linepack}(\rho)} \\ \times \left(h_{l,t}^{\text{linepack}*(\rho)} (\mathbf{Q}_{l,t}^{\text{in}(\rho)}, \mathbf{Q}_{l,t-1}^{\text{in}(\rho)}, \mathbf{Q}_{l,t}^{\text{out}(\rho)}, \mathbf{Q}_{l,t-1}^{\text{out}(\rho)}) \right. \\ \left. + [\nabla h_{l,t}^{\text{linepack}*(\rho)} (\mathbf{Q}_{l,t}^{\text{in}(\rho)}, \mathbf{Q}_{l,t-1}^{\text{in}(\rho)}, \mathbf{Q}_{l,t}^{\text{out}(\rho)}, \mathbf{Q}_{l,t-1}^{\text{out}(\rho)})]^T \right. \\ \left. \times \begin{bmatrix} \mathbf{Q}_{l,t}^{\text{in}} - \mathbf{Q}_{l,t}^{\text{in}(\rho)} \\ \mathbf{Q}_{l,t-1}^{\text{in}} - \mathbf{Q}_{l,t-1}^{\text{in}(\rho)} \\ \mathbf{Q}_{l,t}^{\text{out}} - \mathbf{Q}_{l,t}^{\text{out}(\rho)} \\ \mathbf{Q}_{l,t-1}^{\text{out}} - \mathbf{Q}_{l,t-1}^{\text{out}(\rho)} \end{bmatrix} \right) \leq 0. \quad (58)$$

The non-linear equalities of gas flow equation (19), compressor power consumption (20), and hourly linepack (27) are relaxed to inequalities of (56), (57), and (58), respectively, whereas the master problem is a MILP problem, it can be solved using the standard BB algorithms. The integer cuts are in the form of (59). These integer cuts eliminate the already found binary variables. Therefore, in this method, all 0-1 combinations of the problem are taken into account (see (59)), where $|\mathbf{R}^{(\rho)}|$ is the cardinality of $\mathbf{R}^{(\rho)}$ and

$$\mathbf{R}^{(\rho)} = \{\sigma: \gamma_{\sigma,t,i}^{(\rho-1)} = 1\},$$

$$\mathbf{NR}^{(\rho)} = \{\sigma: \gamma_{\sigma,t,i}^{(\rho-1)} = 0\}.$$

In each iteration, the objective function of the master problem must be within the current objective function of the primal and previous objective value of the master to proceed to convergence (60). The optimisation is terminated when the criterion (61) is satisfied or the

$$\forall \rho \in \mathcal{F}, i \in \mathcal{H}, t \in \mathcal{T}: \sum_{\sigma \in \mathbf{R}^{(\rho)}} \gamma_{\sigma,t,i}^{(\rho)} - \sum_{\sigma \in \mathbf{NR}^{(\rho)}} \gamma_{\sigma,t,i}^{(\rho)} \leq |\mathbf{R}^{(\rho)}| - 1, \quad (59)$$

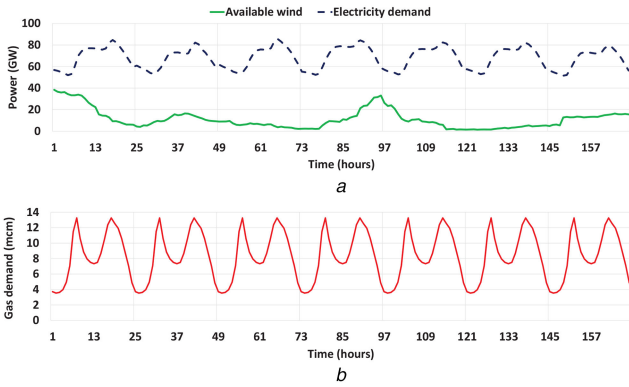


Fig. 7 Input data to the system
(a) Available wind and electricity demand, (b) Gas demand

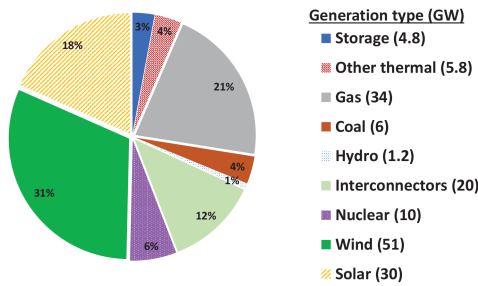


Fig. 8 GB 2030 power generation mix in this study

master problem is infeasible. Parameter ϵ is the convergence bound of the OA/ER approach

$$\forall \rho \in \mathcal{F}: X_{\text{master}}^{(\rho-1)} \leq X_{\text{master}}^{(\rho)} \leq X_{\text{primal}}^{(\rho)}, \quad (60)$$

$$|X_{\text{master}}^{(\rho)} - X_{\text{primal}}^{(\rho)}| \leq \epsilon. \quad (61)$$

4.5 Algorithmic development

The procedure of OA/ER can be described as follows:

- *Step 1:* Setting initial points for $w_{i,t}^{\text{su}(1)}$ and $w_{i,t}^{\text{sd}(1)}$.
- *Step 2:* Solving the primal problem (NLP) and taking the information of $g(Q_i^{\text{supp}*}(\rho), Q_i^{\text{gstor}*}(\rho), CL_i^*(\rho), Q_i^{\text{gshed}*}(\rho)), f(P_i^{*(\rho)}, P_i^{\text{shed}*}(\rho), e_i^{*(\rho)}, ur_i^{*(\rho)}, \lambda_{x,t}^{\text{flow}(\rho)}, \lambda_{x,t}^{\text{comp}(\rho)}, \text{and } \lambda_{x,t}^{\text{linepack}(\rho)}$.
- *Step 3:* Calculating $\Phi_{x,t}^{\text{flow}(\rho)}, \Phi_{x,t}^{\text{comp}(\rho)}, \text{and } \Phi_{x,t}^{\text{linepack}(\rho)}$.
- *Step 4:* Calculating the required terms for (55)–(58).
- *Step 5:* Solving the relaxed master problem (MILP). If the master problem is feasible then taking the information of $w_{i,t}^{\text{su}*}(\rho)$ and $w_{i,t}^{\text{sd}*}(\rho)$ for the next iteration of primal.
- *Step 6:* If (60) is satisfied or the master problem is infeasible then terminate. Otherwise, return to step 1.

5 Case studies

The operation of a GB natural gas and power systems is modelled for a winter week considering high electricity demand and variabilities in wind generation in 2030. The interaction between natural gas and power systems is quantified through using coupled and decoupled operation strategies for these systems. Afterwards, the role of natural gas system related flexibilities in the interaction between natural gas and power systems is evaluated. In this study, options of (a) more flexible gas-fired plants (FlexGPs) [30]; where about 30% of the existing gas plants can operate more flexible, (b) flexible compressors [34]; where the one-directional compressors

are replaced with multi-directional ones, and (c) increasing the gas imports to the gas system are taken into account.

5.1 GB natural gas and power systems

The demand and available wind for a winter week are presented in Fig. 7. The historical hourly electricity demand is obtained from the National Grid and scaled up to represent 2030. Due to the projection of electrification of heat and transport sectors [40], the peak demand is assumed to be 85 GW. Real hourly wind generation data observed in GB during 15 April 2013–22 April 2013 [41] is scaled up to represent the wind generation in 2030 [30].

In this study, a period of a sudden drop in wind and increase in electricity demand is considered as well to evaluate how the system deals with a dramatic increase in net demand (98–118 h). Additionally, partial unavailability of gas terminals throughout the week due to maintenance is assumed in this study. The model is implemented on a natural gas system and 29-busbar power transmission system presented in [34]. The power generation mix is derived from [40]. In Fig. 8, it is shown that around 50% of the power is provided by renewable technologies.

5.2 Description of case studies

To investigate the role of the mentioned flexibility options in the interaction of natural gas and power systems, the following case studies are considered:

- *Base:* In the Base case, no significant means of flexibility are introduced to the system.
- *FlexGP:* It is assumed that 30% of gas-fired generation capacity is operationally more flexible [30].
- *Flexible compressors (Multi):* Compressors are able to boost pressure in multiple directions [34].
- *Gas imports (Int-5% and Int-10%):* Increasing the gas supply through importing 5 and 10% more gas from outside GB.
- *All flexible (Flex-5% and Flex-10%):* In these cases, all above-mentioned flexibility options with 5 and 10% increased gas imports is considered.

These cases are derived to see how different flexibility options related to the natural gas system, including flexibilities provided to the natural gas system infrastructure and more FlexGPs can smooth the interaction between natural gas and power systems.

6 Key findings of the proposed models

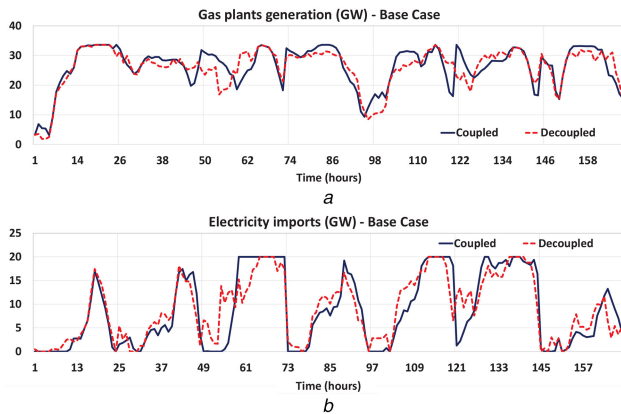
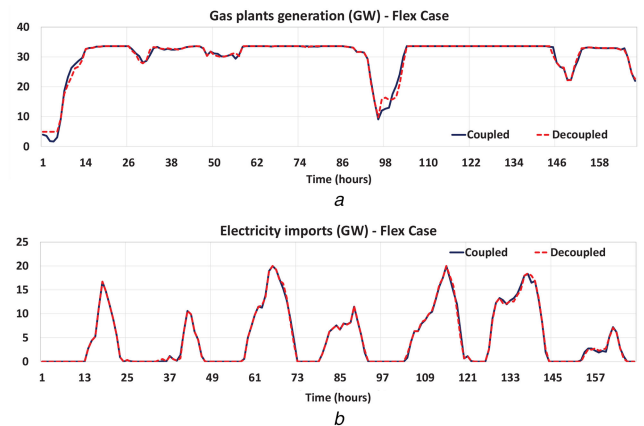
6.1 Computational performance

The corresponding optimisation problem of operation of natural gas for the entire week contains around 260k variables including 20k integer variables. Due to the rolling approach, the model is broken down into seven smaller optimisation problems. As mentioned previously, 32 h are optimised in each of these optimisation problems. Therefore, at each step around 50k variables including 4k integer variables are optimised.

From modelling perspectives, in both coupled and decoupled models, MILP and NLP problems are optimised. However, since in the decoupled model, the natural gas and power systems are optimised separately, the number of variables in each problem is less than the coupled model and hence the convergence should be faster. For example, in the Base case, the computation time of the first iteration is 88.9 min. However, according to Fig. 3, in case of gas load shedding the model should be run for the next iteration. Hence, overall the computation time of the decoupled model is more than the coupled model. The computational performance of the coupled and decoupled models in different case studies for the entire week is provided in Table 1. As is presented, the coupled

Table 1 Approximated computational performance in minutes

Modelling	Base	Multi	Int-5%	FlexGP	Flex-5%	Int-10%	Flex-10%
decoupled	245	232	261	235	240	238	234
coupled	130	114	117	90	101	98	115

**Fig. 9** Electricity supply in Base case: (a) Electricity produced by gas plants, (b) Electricity imports**Fig. 10** Electricity supply in Flex-10% case: (a) Electricity produced by gas plants, (b) Electricity imports**Table 2** Aggregated generated electricity by gas plants in coupled mode in GWh

Base	Multi	Int-5%	FlexGP	Flex-5%	Int-10%	Flex-10%
26.2	25.5	27.1	28.6	27.3	29.4	30.1

model (two iterations) performance is 88–161% faster than the decoupled (up to two iterations) model through different case studies.

To demonstrate the value of the flexibility options in the interaction of natural gas and power system, the presence of these options in coupled and decoupled modelling of operation of natural gas and power systems are quantified. In this section, the key numerical results are presented.

6.2 Power system analysis

In Fig. 9a, gas plants generation scheduling in the Base case for both operation strategies is presented. It is shown that especially in 98–118 h, in the coupled approach, more power is produced by the gas plants. The reason is that since in this model, all the security of supply constraints are considered simultaneously, the gas plants are scheduled so that to compensate for the lack of wind more appropriately. On the other hand, in the decoupled approach, due to the partial unavailability of gas supply terminals along with the fact the gas transmission in the grid is relatively slow, the gas could not be delivered to some of the gas plants. Consequently, as shown in Fig. 9b, to keep the supply–demand balance, more electricity is imported (i.e. more expensive option).

If the systems become more flexible, this leads to better operation in the decoupled mode. As it can be illustrated from Fig. 10, if there is enough flexibility in the systems, including flexible gas plants, multi-directional compressors, and more flexibility in the gas interconnectors, the gas plants scheduling in both operational strategies are relatively close to each other. This is due to the fact that, in the natural gas system, the gas transportation system is improved, and therefore the gas could be delivered to the gas plants as required. In the power system, thanks to the provided flexibility in the gas plants, the flexibility of the natural gas system is reflected in the power system, and as a result re-dispatching of these plants in the decoupled mode is done properly.

In Table 2, the electricity generated by the gas-fired plants in all of the case studies in coupled mode is presented. It is demonstrated that if flexibility is provided, the produced electricity by gas-fired plants is increased. This is due to (a) reinforcement in natural gas infrastructure, which leads to improved gas system delivery to the gas plants (Multi case), (b) more availability of gas supply (Int-5% and Int-10% cases), and (c) improved generation characteristics

(e.g. ramp up/down, minimum up time/minimum down time (MUT/MDT), minimum stable generation (MSG), and efficiency) of the gas plants (FlexGP case). As expected, in case of Flex-10%, the most electricity produced by the gas plants is achieved in order to facilitate the energy-supply balance.

6.3 Natural gas system analysis

In Fig. 11, the aggregated linepack in the pipelines for the time period where significant changes in electricity net demand and gas demand happen (i.e. 87–106 h), is presented. It is shown how the linepack will deal with the dynamics of the system. In the case of an increase in electricity and gas demand, the linepack will help to deliver the gas to the gas plans for electricity generation as well as non-electric gas demands. Furthermore, in case of demand decrease, more gas is stored in the pipelines to deal with the next rapid change in the system.

In Table 3, it is presented that if the flexibility of the energy system is increased, more linepack is available throughout the day. This enables the gas system operator to deal more properly with the rapid changes in the system. However, it is demonstrated that in the coupled model, since the whole-system constraints are taken into account, the flexibility provided by the gas system is more used compared to the same case in the decoupled model.

To highlight the operation of the natural gas system, the gas supply–demand balance criteria is presented. In Table 4, it is demonstrated that in the decoupled approach, due to the operational limitations in the gas delivery in the transmission grid, the gas could not be delivered to some of the gas demands. It is shown that if the systems become more flexible, the gas delivery is improved and finally, in the most flexible case that is considered in this study (Flex-10% case), there is no need to shed any gas demands. In coupled modelling, since all the constraints of the systems are taken into account at the same time, gas demand curtailment has not happened.

6.4 Operational cost of natural gas and power systems

In Fig. 12, the operational cost difference of natural gas and power systems in the decoupled approach in respect to the coupled approach is shown. It can be concluded if there is no flexibility provided in the systems, the proposed decomposition method for

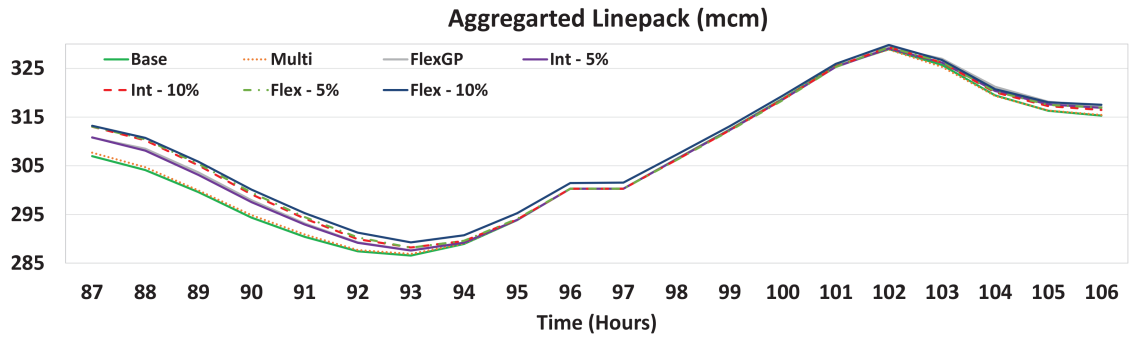


Fig. 11 Available linepack in the pipelines in different cases for the coupled mode

Table 3 Average linepack in the pipelines (mcm)

Modelling	Base	Multi	Int-5%	FlexGP	Flex-5%	Int-10%	Flex-10%
decoupled	310.9	311.2	311.2	311.2	311.1	311.3	313.5
coupled	309.7	309.6	310.2	310.2	310.1	310.8	311.4

Table 4 Gas load shedding (mcm)

Modelling	Base	Multi	Int-5%	FlexGP	Flex-5%	Int-10%	Flex-10%
decoupled	7.22	4.24	4.73	1.83	0.73	0.12	—
coupled	—	—	—	—	—	—	—

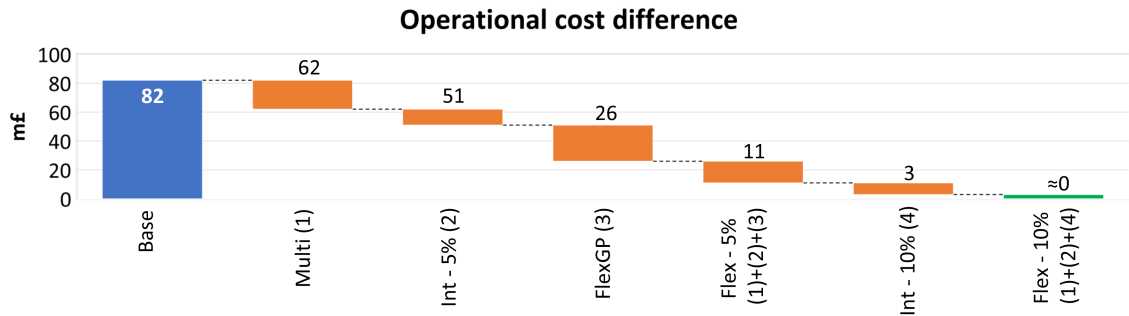


Fig. 12 Natural gas and power systems operational cost difference of decoupled mode in respect to the coupled mode

solving effectively the coupled strategy results in up to 7% cost saving (operational cost of the Base case in coupled mode is £1081m). On the other hand, once the systems become more flexible, the cost differences are becoming smaller. Finally, if there is enough flexibility in natural gas and power systems, the systems are operated in the decoupled model, very close to the coupled approach.

7 Conclusion

In order to solve efficiently the MINLP problem of the coordinated operation of coupled natural gas and power systems, to the best of our knowledge, for the first time, an OA/ER decomposition method was applied to the model. The value of the proposed coupled operational modelling of natural gas and power systems was quantified through comparing with the decoupled modelling of these systems. It was shown that in the coupled approach the systems were operating more cost-effectively (i.e. 7% cost saving). This indicates that the coupled modelling could enhance the flexibility of the system and enables control of natural gas and power systems more efficiently to deal with the variabilities of the renewable energy sources (RES) in order to meet the supply-demand balance.

Afterwards, the options of flexible compressors, flexible gas plants, and gas interconnections were employed in the system, to make the natural gas and power systems more flexible. It was demonstrated that by making the systems more flexible, the value of the coupled modelling was decreased since in the decoupled approach the operation of natural gas and power systems was improved. Finally, if we have all the mentioned options in the systems, the operation of the natural gas and power systems were

almost the same as the coupled operation of these systems. As a result, it could be concluded that if the systems are flexible enough, a decoupled modelling of these systems can meet the required constraints.

This becomes important, since for a coupled operation of these systems, reforming the current regulatory and market framework to coordinate the operation of natural gas and power systems is required, which needs revisions in high-level energy policies in different countries. On the other hand, to have these options in the system, the investment costs should also be taken into account. Therefore capital cost of the flexibility options will play an important role in the future decision-making of the energy systems.

8 Acknowledgments

The authors gratefully acknowledge the “Sustainable gas pathways for Brazil; from microcosm to macrocosm” project for providing funding for this work under NERC grant NE/N018656/1.

9 References

- [1] MacLeay, I., Harris, K., Annut, A., et al.: ‘Digest of United Kingdom energy statistics 2015’ (Department of Energy and Climate Change, London, 2015)
- [2] Committee of Climate Change (CCC): ‘The fifth carbon budget – the next step towards a low-carbon economy’, Committee on Climate Change, 2015
- [3] Oswald, J., Raine, M., Ashraf-Ball, H.: ‘Will British weather provide reliable electricity?’, *Energy Policy*, 2008, 36, (8), pp. 3212–3225
- [4] Liu, C., Shahidehpour, M., Fu, Y., et al.: ‘Security-constrained unit commitment with natural gas transmission constraints’, *IEEE Trans. Power Syst.*, 2009, 24, (3), pp. 1523–1536
- [5] Zhang, X., Shahidehpour, M., Alabdulwahab, A., et al.: ‘Hourly electricity demand response in the stochastic day-ahead scheduling of coordinated electricity and natural gas networks’, *IEEE Trans. Power Syst.*, 2016, 31, (1), pp. 592–601

- [6] Chaudry, M., Jenkins, N., Strbac, G.: 'Multi-time period combined gas and electricity network optimisation', *Electr. Power Syst. Res.*, 2008, **78**, (7), pp. 1265–1279
- [7] Correa-Posada, C.M., Sanchez-Martin, P.: 'Integrated power and natural gas model for energy adequacy in short-term operation', *IEEE Trans. Power Syst.*, 2015, **30**, (6), pp. 3347–3355
- [8] Sardou, I.G., Khodayar, M.E., Ameli, M.T.: 'Coordinated operation of natural gas and electricity networks with microgrid aggregators', *IEEE Trans. Smart Grid*, 2018, **9**, (1), pp. 199–210
- [9] Correa-Posada, C.M., Sanchez-Martin, P.: 'Security-constrained optimal power and natural-gas flow', *IEEE Trans. Power Syst.*, 2014, **29**, (4), pp. 1780–1787
- [10] Gil, M., Duenas, P., Reneses, J.: 'Electricity and natural gas interdependency: comparison of two methodologies for coupling large market models within the European regulatory framework', *IEEE Trans. Power Syst.*, 2016, **31**, (1), pp. 361–369
- [11] Zlotnik, A., Roald, L., Backhaus, S., *et al.*: 'Coordinated scheduling for interdependent electric power and natural gas infrastructures', *IEEE Trans. Power Syst.*, 2017, **32**, (1), pp. 600–610
- [12] Clegg, S., Mancarella, P.: 'Integrated modeling and assessment of the operational impact of power-to-gas (P2G) on electrical and gas transmission networks', *IEEE Trans. Sustain. Energy*, 2015, **6**, (4), pp. 1–11
- [13] Ameli, H., Qadrdan, M., Strbac, G.: 'Techno-economic assessment of battery storage and power-to-gas: a whole-system approach', *Energy Procedia*, 2017, **142**, pp. 841–848. Proceedings of the 9th International Conference on Applied Energy
- [14] Floudas, C.A.: '*Nonlinear and mixed-integer optimization: fundamentals and applications*' (Oxford University Press, USA, 1995)
- [15] Bussieck, M.R., Pruessner, A.: '*Mixed-integer nonlinear programming*' (GAMES Development Corporation, Halifax, 2003)
- [16] Senjyu, T., Shimabukuro, K., Uezato, K., *et al.*: 'A fast technique for unit commitment problem by extended priority list', *IEEE Trans. Power Syst.*, 2003, **18**, (2), pp. 882–888
- [17] Chen, C.L., Wang, S.C.: 'Branch-and-bound scheduling for thermal generating units', *IEEE Trans. Energy Convers.*, 1993, **8**, (2), pp. 184–189
- [18] Ongsakul, W., Petcharakas, N.: 'Unit commitment by enhanced adaptive Lagrangian relaxation', *IEEE Trans. Power Syst.*, 2004, **19**, (1), pp. 620–628
- [19] Frangioni, A., Gentile, C., Lacalandra, F.: 'Tighter approximated MILP formulations for unit commitment problems', *IEEE Trans. Power Syst.*, 2009, **24**, (1), pp. 105–113
- [20] Murillo-Sanchez, C., Thomas, R.J.: 'Thermal unit commitment with nonlinear power flow constraints'. IEEE Power Engineering Society 1999 Winter Meeting (Cat. No.99CH36233), New York, 1999, vol. 1, pp. 484–489
- [21] Ameli, H., Ameli, M.T., Hosseini, S.H.: 'Multi-stage frequency control of a microgrid in the presence of renewable energy units', *Electr. Power Compon. Syst.*, 2017, **45**, (2), pp. 159–170
- [22] Nasri, A., Kazempour, S.J., Conejo, A.J., *et al.*: 'Network-constrained ac unit commitment under uncertainty: a benders decomposition approach', *IEEE Trans. Power Syst.*, 2016, **31**, (1), pp. 412–422
- [23] Chung, C.Y., Yu, H., Wong, K.P.: 'An advanced quantum-inspired evolutionary algorithm for unit commitment', *IEEE Trans. Power Syst.*, 2011, **26**, (2), pp. 847–854
- [24] Ameli, H., Abbasi, E., Ameli, M.T., *et al.*: 'A fuzzy-logic based control methodology for secure operation of a microgrid in interconnected and isolated modes', *Int. Trans. Electr. Energy Syst.*, 2017, **27**, (11), p. e2389
- [25] Jeong, Y.W., Park, J.B., Jang, S.H., *et al.*: 'A new quantum-inspired binary PSO: application to unit commitment problems for power systems', *IEEE Trans. Power Syst.*, 2010, **25**, (3), pp. 1486–1495
- [26] Shao, C., Wang, X., Shahidehpour, M., *et al.*: 'An MILP-based optimal power flow in multicarrier energy systems', *IEEE Trans. Sustain. Energy*, 2017, **8**, (1), pp. 239–248
- [27] Dai, C., Wu, L., Wu, H.: 'A multi-band uncertainty set based robust SCUC with spatial and temporal budget constraints', *IEEE Trans. Power Syst.*, 2016, **31**, (6), pp. 4988–5000
- [28] Ruiz, J.P., Wang, J., Liu, C., *et al.*: 'Outer-approximation method for security constrained unit commitment', *IET Gener. Transm. Distrib.*, 2013, **7**, (11), pp. 1210–1218
- [29] Qadrdan, M., Chaudry, M., Wu, J., *et al.*: 'Impact of a large penetration of wind generation on the GB gas network', *Energy. Policy*, 2010, **38**, (10), pp. 5684–5695
- [30] Qadrdan, M., Ameli, H., Strbac, G., *et al.*: 'Efficacy of options to address balancing challenges: integrated gas and electricity perspectives', *Appl. Energy*, 2017, **190**, pp. 181–190
- [31] Deane, J.P., Ciarain, M.O., Gallachoir, B.P.O.: 'An integrated gas and electricity model of the EU energy system to examine supply interruptions', *Appl. Energy*, 2017, **193**, pp. 479–490
- [32] He, C., Wu, L., Liu, T., *et al.*: 'Robust co-optimization scheduling of electricity and natural gas systems via ADMM', *IEEE Trans. Sustain. Energy*, 2017, **8**, (2), pp. 658–670
- [33] Osiadacz, A.: '*Simulation and analysis of gas networks*' (Gulf Publishing Company, Houston, 1987)
- [34] Ameli, H., Qadrdan, M., Strbac, G.: 'Value of gas network infrastructure flexibility in supporting cost effective operation of power systems', *Appl. Energy*, 2017, **202**, pp. 571–580
- [35] Wood, A.J., Wollenberg, B.F.: '*Power generation, operation, and control*' (Wiley, New York, USA, 1996)
- [36] Gröwe-Kuska, N., Kiwiel, K.C., Nowak, M.P., *et al.*: 'Power management in a hydro-thermal system under uncertainty by Lagrangian relaxation'. Decision Making Under Uncertainty: Energy and Power, 2002, pp. 39–70
- [37] Qadrdan, M., Wu, J., Jenkins, N., *et al.*: 'Operating strategies for a GB integrated gas and electricity network considering the uncertainty in wind power forecasts', *IEEE Trans. Sustain. Energy*, 2014, **5**, (1), pp. 128–138
- [38] 'Fico xpress optimisation suite'. Available at http://www.maths.ed.ac.uk/hall/Xpress/FICO_Docs/mosel/mosel_lang/dhtml/moselref.html
- [39] Grossmann, I.E.: 'Review of nonlinear mixed-integer and disjunctive programming techniques', *Optim. Eng.*, 2002, **3**, (3), pp. 227–252
- [40] National Grid plc, 'Future energy scenarios: system operator' (National Grid plc, Warwick, 2018)
- [41] 'Elexon Ltd'. Available at <http://www.Elexon.co.uk>, accessed 01 January 2013